Heats of Formation of $HCCl_3$, $HCCl_2Br$, $HCClBr_2$, $HCBr_3$, and Their Fragment Ions Studied by Threshold Photoelectron Photoion Coincidence

Nicholas S. Shuman, Linda Ying Zhao, Michael Boles, and Tomas Baer*

Department of Chemistry, University of North Carolina, Chapel Hill, North Carolina 27599-3290

Bálint Sztáray

Department of Chemistry, University of the Pacific, Stockton, California 95211

Received: June 26, 2008; Revised Manuscript Received: August 19, 2008

The dissociative photoionization onsets for Cl and Br loss reactions were measured for $HCCl_3$, $HCCl_2Br$, $HCClBr_2$, and $HCBr_3$ by threshold photoelectron photoion coincidence (TPEPICO) in order to establish the heats of formation of the mixed halides as well as the following fragment ions: $HCCl_2^+$, $HCClBr^+$, $HCBr_2^+$. The first zero Kelvin onsets were measured with a precision of 10 meV. The second onsets, which are in competition with the lower energy onsets, were established with a precision of 60 meV. Because both the chloroform and bromoform have relatively well established heats of formation, these measurements provide a route for establishing the heats of formation of the mixed halomethanes within uncertainties of less than 5 kJ mol^{-1}.

Introduction

A confluence of factors has generated considerable interest in recent years in establishing highly accurate heats of formation and bond energies. Among these are the advances in quantum mechanical calculations, which are now capable of achieving ± 1 kJ mol^{-1} accuracy for small molecules.[1−5] Because the number of quantum calculations seem to be rising rapidly, it is important for high-quality experimental results to keep pace in order test the reliability of these calculations. The second major factor is the emergence of the active thermochemical tables,[6,7] an interactive network that includes both experimental data as well as theoretical calculations and that is capable of automatically updating all values when newer values are entered. Because experimental values refer only to differences in energies, any change in a reference value will change all the derived values anchored upon it. Additionally, where redundant measurements exist, it is desirable to statistically evaluate all results in order to spot outliers and provide better accuracy and more appropriate (and hopefully lower) uncertainty. These are arduous tasks for a researcher working from the literature or a static compilation of thermochemical data, but the active tables do them automatically.

Alkyl halides, especially the bromines and iodides, have traditionally been among the more difficult molecules to calculate because of the large number of electrons associated with the halogen and because relativistic effects become important for these high-mass atoms. On the other hand, such factors do not affect the experimental measurements.

We have recently embarked on photoionization studies of alkyl halides using the technique of threshold photoelectron photoion coincidence (TPEPICO), which permits us to energy-select ions and to determine accurate dissociation onsets for reactions such as $AB + h\nu \rightarrow A^+ + B^\bullet + e^-$. If we know the heats of formation of two of the species, the third one can be determined. The first set of molecules investigated were the methyl dihalides, H_2CXY, X, Y = Cl, Br, and I.[8] With the use of H_2CCl_2 as an anchor, it was possible to establish the heats of formation of all the dihalomethane molecules. Other studies involved vinyl bromide and 1,1,2-tribromoethane,[9] vinyl chloride and vinyl iodide, and chloroform and 1,1,2,2-tetrachloroethane.[10] In the present study, we investigate the methyl trihalides, HCX_nY_{3-n}, X, Y = Cl, Br. The iodo derivatives were not included because some of them are not commercially available.

The following reaction onsets were to be determined experimentally:

$$CHCl_3 + h\nu \xrightarrow{E_{01}} CHCl_2^+ + Cl\cdot + e^- \quad (1)$$

$$CHCl_2Br + h\nu \xrightarrow{E_{02}} CHCl_2^+ + Br\cdot + e^- \quad (2)$$

$$\xrightarrow{E_{03}} CHClBr^+ + Cl\cdot + e^- \quad (3)$$

$$CHClBr_2 + h\nu \xrightarrow{E_{04}} CHClBr^+ + Br\cdot + e^- \quad (4)$$

$$\xrightarrow{E_{05}} CHBr_2^+ + Cl\cdot + e^- \quad (5)$$

$$CHBr_3 + h\nu \xrightarrow{E_{06}} CHBr_2^+ + Br\cdot + e^- \quad (6)$$

In order to obtain heats of formation of the various intermediate species, it is important to have firm values upon which to anchor the measurements. The heat of formation of $CHCl_3$ has been well established at -102.9 ± 2.5 kJ mol^{-1} by a 2002 review by Manion,[11] based primarily on a rotating bomb calorimetry measurement.[12] A recent theoretical calculation by Lazarou et al.[13] carried out at the CCSD(T) level with extrapolation to the complete basis set reported a value of -102.6 ± 0.6 kJ mol^{-1}. The bromoform heat of formation is less well established, with experimental values ranging from 17 kJ mol^{-1} by Wagman et al.,[14] 23.8 ± 4.5 kJ mol^{-1} in Pedley,[15] to 55.4 $\pm$ 3.3 kJ mol^{-1} obtained by rotating bomb calorimetry by Papina et al.[16] There is somewhat less spread among the calculated values. A 2004 CCSD(T) calculation with relativistic corrections

* Corresponding author.

10.1021/jp8056459 CCC: $40.75
Published on Web 09/30/2008

by Oren et al.[17] reported a 298 K heat of formation of 54.3 kJ mol^{-1}, which agrees quite nicely with the Papina value. Marshall et al. report a QCISD(T) value of 51.6 ± 3 kJ mol^{-1},[18] and a very recent theoretical study using G3X without relativistic corrections reported two values based on isodesmic reactions, with an average of 45.8 ± 2.3 kJ mol^{-1}.[19] The bromoform values clearly have not yet converged to a consensus value. However, given agreement between the highest level calculation of Oren et al. and the rotating bomb calorimetry value of Papina et al., we will assume a value of 55.0 ± 6 kJ mol^{-1}.

The heats of formation of the mixed trihalomethanes and the ionic fragments are much less well established. We could find no experimental values for the heats of formation of $CHClBr_2$ and of $CHCl_2Br$, which is surprising considering the importance of these molecules in atmospheric chemistry. Their heats of formation are estimated by Gurvich et al. to be −45 and 10 kJ mol^{-1}, respectively, at 298 K, however with uncertainties greater than 10 kJ mol^{-1}.[20] The $CHCl_2^+$ heat of formation has been previously determined by TPEPICO to be 888.9 ± 1.3 kJ mol^{-1} at 298 K.[10] The $CHBr_2^+$ heat of formation can be derived from the heat of formation and adiabatic ionization energy of $CHBr_2^•$ to be 987 kJ mol^{-1} albeit with a substantial uncertainty of at least 10 kJ mol^{-1}.[21,22] An experimental[23] value for the $CHClBr^•$ 298 K heat of formation does exist; however, there is no reported ionization energy and we can derive no value for the $CHClBr^+$ heat of formation.

In this work, the 0 K dissociation onsets of reactions 1−6 are measured and used to derive the heats of formation of all of these compounds relative to the $CHCl_3$ heat of formation and, entirely independently, relative to the $CHBr_3$ heat of formation.

Experimental Approach

The details of the TPEPICO spectrometer have been described previously.[24−26] The samples of $CHCl_3$, $CHBr_3$, $CHCl_2Br$, and $CHClBr_2$ were purchased from Sigma-Aldrich and were introduced at room temperature into the ionization region through a needle. The molecules were ionized with vacuum ultraviolet (VUV) light generated from a hydrogen discharge lamp and dispersed by a 1 m normal incidence monochromator. The entrance and exit slits of the monochromator are set to 100 μm, which resulted in a resolution of 1 Å (about 10 meV at 10 eV photon energy). The photon energy scale was calibrated using the hydrogen Lyman-α resonance line. The electrons and ions were extracted in opposite directions in an applied field of 20 V cm^{-1}.

Threshold electrons were velocity focused by extraction with gridless apertures in a 13 cm drift tube set to 77 V through a 1.3 mm aperture onto a channeltron detector.[24] The hot electron signal, which contaminates the threshold electron signal, was subtracted by collecting off axis hot electron coincidences as described by Sztáray and Baer.[25] The ions were directed either to a linear time-of-flight (TOF) mass spectrometer or to a reflectron (RETOF). The RETOF consists of a single 5 cm acceleration region, followed by a 40 cm drift region, a 15 cm reflectron section, and last a second 30 cm drift region. In the linear TOF, ions were first accelerated over a 5 cm acceleration region, then a 5 mm second acceleration region, and finally drifted across a 34 cm field-free region. In both the RETOF and the linear TOF, ions were detected with microchannel plates (MCPs) at the end of the drift region. The bromoform and the bromine loss from $CHBr_2Cl$ measurements were carried out using the RETOF, while all other data were taken with the linear TOF setup. Because the ions from the trihalomethane compounds dissociate rapidly (i.e., are not metastable) and the ion mass peaks were readily resolved in both setups, results from RETOF and linear TOF are expected to be identical. The setup used for each compound was determined solely by the current availability of the apparatus.

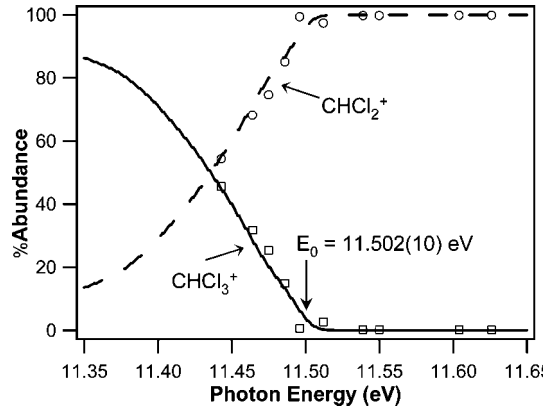

Figure 1. Breakdown diagram of $CHCl_3^+$. Points are experimentally measured ion abundances, and lines are the best-fit modeling of the data (see text). The determined 0 K dissociation onset is shown with the uncertainty of the final digits in parentheses.

The electron and ion signals served as the start and stop signal for a time to pulse height converter, which generates the TOF spectrum. All of the halomethane ions dissociate rapidly on the time scale of ion extraction so that their TOF peaks are symmetric and sharp. The only information we obtain from these data is the relative abundance of the parent and fragment ions. Because only the peak areas are of interest in the fast dissociation, in order to correct for hot electron contamination we simply multiply the hot electron TOF peaks by a constant factor (usually about 0.16) and subtract it from the center spectrum. This factor is obtained by taking the ratio of the parent ion peaks for the center and off-center spectra at a photon energy well in excess of the dissociation limit, where no parent ion should be present. Once established, this factor remains constant for the whole analysis and, in general, remains constant from one molecule to the next. It can change if the collection efficiency of one of the detectors changes.

Vibrational frequencies required for Rice−Ramsberger−Kassel−Marcus (RRKM) analysis of the experimental breakdown diagrams were determined using the Gaussian 03 quantum chemical code.[27] at the B3LYP/6-311++G** level. No scaling factor was applied. Transition state frequencies were calculated by a constrained optimization with the [carbon-leaving halogen] bond stretched to about 4.0 Å.

Results and Discussion

The breakdown diagrams, which are the relative ion abundances as a function of the photon energy, for the four trihalomethane ions are shown in Figures 1−4. Note that in two cases, $CHCl_3$ and $CHCl_2Br$, the breakdown diagrams appear incomplete at lower photon energies. When the photon energy equals the ionization energy of these molecules a significant portion of the ions are already produced with sufficient energy to dissociate, resulting in a significant abundance of daughter ions. At lower photon energies the number of ions created decreases drastically; the data become subject to experimental artifacts and have as a result been omitted from the analysis. In the case of the chloro- and bromoform ions only a single dissociation channel is observed, whereas in the mixed trihalides a competitive halogen loss channel opens up at higher energies.

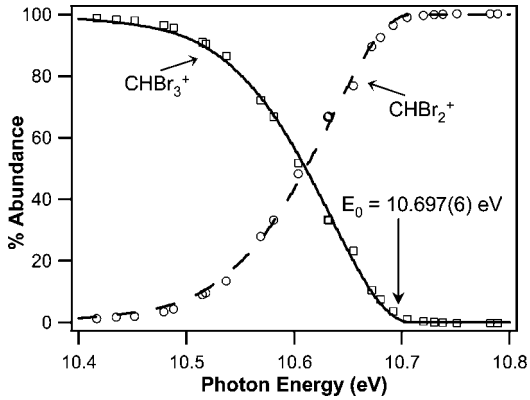

Figure 2. Breakdown diagram for $CHBr_3^+$.

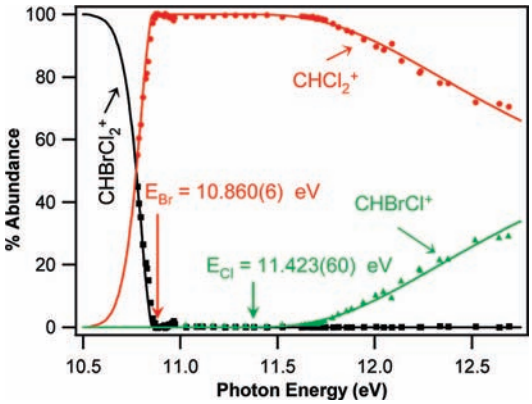

Figure 3. Breakdown diagram for $CHCl_2Br^+$. Parent ion abundances are shown in black, Br loss daughter ion abundances are in red, and Cl loss daughter ion abundances are in green.

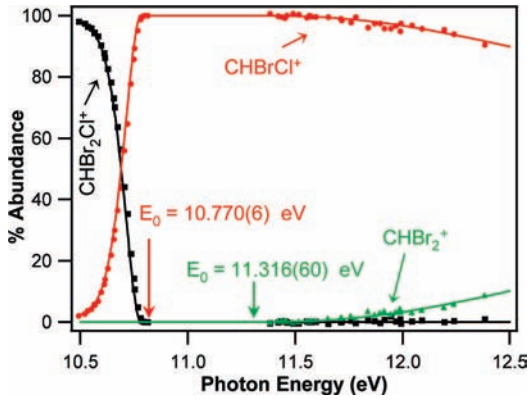

Figure 4. Breakdown diagram for $CHClBr_2^+$. Parent ion abundances are shown in black, Br loss daughter ion abundances are in red, and Cl loss daughter ion abundances are in green.

In modeling the first dissociation onset, a single parameter, the dissociation energy at 0 K, E_0, is required to obtain the fit. Because the sample is at room temperature, we begin with a thermal energy distribution, $P(\varepsilon)$, so that the total energy of an "energy-selected" ion is $h\nu + \varepsilon$, where ε is the thermal energy in the molecule prior to being ionized. If the dissociation is fast on the time scale of the experiment (as is the case for all the dissociations here), then any ion whose energy $E = h\nu + \varepsilon < E_0$ will dissociate. If it is less than E_0, it will remain as a parent ion. Thus, the modeling of the data just involves integrating the thermal energy distribution and varying the assumed E_0 until a best fit to the experimental data is obtained. The $P(\varepsilon)$ function can be calculated by $P(\varepsilon) = \rho(E)e^{-E/kT}$, where k is the Boltzmann constant, T is the sample temperature, and $\rho(E)$ is the molecule's density of states at an energy E and is calculated using the molecule's vibrational frequencies and rotational constants determined by density functional theory (DFT) calculations. It is evident that the E_0 should be in the vicinity of disappearance of the parent ion because, at that energy, all of the ion's thermal energy distribution lies above the dissociation limit. These best fits to the breakdown diagrams are indicated in Figures 1−4.

The onset for Cl loss from the chloroform has been measured several times. An old photoionization value of Werner et al. reported 11.49 ± 0.020 eV,[28] whereas Lago and Baer, using the current instrument, found 11.50 ± 0.007 eV.[10] A much higher resolution pulsed field ionization PEPICO value of 11.488 ± 0.002 eV was reported by Lau and Ng, all of which agree well with the present value of 11.502 ± 0.010 eV. The Br loss onset from bromoform has been reported once by Tsai et al., who found 10.70 ± 0.020 eV,[29] which also is in agreement with our value of 10.697 ± 0.006 eV.

In the cases of the mixed halomethanes, the second onsets (Cl loss) are in competition with the first onsets (Br loss) and must be modeled by taking into account the relative rates of the two dissociation paths. According to the statistical theory of dissociation, RRKM,[30] the rate constant is given by

$$k(E) = \frac{\sigma N^{\ddagger}(E - E_0)}{h\rho(E)} \qquad \text{(I)}$$

where $N^{\ddagger}$ is the transition state sum of states from 0 to $E - E_0$, σ is the reaction degeneracy, h is Planck's constant, and $\rho(E)$ is the ion's density of states. We do not know the absolute rates because they are faster than we can measure; however, of importance in the competitive process are the relative rates for Cl and Br loss. We can calculate the relative rates, expressed as Cl loss over Br loss products, which are equal to the ratio of the ion signals as

$$\frac{[\mathrm{Cl}]}{[\mathrm{Br}]} = \frac{\sigma_{\mathrm{Cl}}}{\sigma_{\mathrm{Br}}} \frac{N^{\ddagger}_{\mathrm{Cl}}(E - E_{\mathrm{Cl}})}{N^{\ddagger}_{\mathrm{Br}}(E - E_{\mathrm{Br}})} \qquad \text{(II)}$$

where the onset energies for the Cl and Br loss channels are given by E_{Cl} and E_{Br}. The onset energy for the lower energy Br loss channel is determined from the first onset as described above. (The determination of the second onset for both $CHCl_2Br^+$ and $CHClBr_2^+$ is essentially invariant of the value used for the first onset. In the case of $CHClBr_2$ E_{Cl} varies by just 3 meV as E_{Br} is varied by 10 meV from the best-fit value.) However, in order to model the ratio of the rates, we need to vary two parameters, which are the onset energy for the Cl loss channel as well as the two lowest transition state frequencies for the Cl loss channel. The latter will affect primarily the slope of the Cl and Br loss curves around the second dissociation onset. At the onset energy for the Cl loss channel, the sum of states in the numerator is $N^{\ddagger}_{\mathrm{Cl}}(0) = 1$. That is, the only way to pass through the transition state is for all the energy to be located in the reaction coordinate and no energy left over for other vibrations or rotations. However, at this energy, the number of open paths for Br loss is equal to $\sigma_{\mathrm{Br}}N^{\ddagger}_{\mathrm{Br}}(E - E_{\mathrm{Cl}})$, which can be several thousand. Thus, the Cl onset will not be evidenced by a step in the breakdown diagram but rather by a shallow curve appearing at an energy above E_{Cl} and with a slope determined by the relative rates of the competing reactions.

In calculating the breakdown diagram in the vicinity of the second onset, we fix the transition state of the Br loss channel by calculating the vibrational frequencies of an ion with the C−Br bond stretched to about 4 Å. Their precise values do not

TABLE 1: Effect of the Assumed Br Loss Channel Activation Entropy on Best-Fit Cl Loss Channel Onset in the Dissociation of $CHBrCl_2^+$

$\Delta S^\ddagger$ at 600 K (J mol^{-1} K^{-1})				
Br loss	Cl loss	$\Delta\Delta S^\ddagger$ (J mol^{-1} K^{-1})	error × 10^{-3} [a]	E_{Cl} (eV)
40.1	49.3	9.2	6.15	11.411
28.6	37.8	9.2	6.15	11.411
17.5	27.2	9.7	6.15	11.419
10.9	20.5	9.6	6.15	11.418
2.4	12.1	9.7	6.15	11.419

[a] See text for definition.

really matter. In the case of the reaction, $HCCl_2Br^+ \rightarrow HCCl_2^+ + Br$, the molecular ion has nine vibrational modes, the transition state has eight modes plus the reaction coordinate, and the final product ion has just six modes. That is, six modes are conserved, one, the C−Br stretch, is the reaction coordinate, and the two C−Br bends are the disappearing modes (these two modes are being converted into rotational motions of the separating fragments). The transition state sum of states is primarily determined by the value of the low-energy disappearing bending mode frequencies, which we fix for the Br loss channel by the DFT calculation. To fit the Cl loss channel data, we simply vary a scaling factor for the two C−Cl bending mode frequencies along with the E_{Cl} onset energy until we get a best fit to the breakdown diagram.

We have tested the above procedure by varying the two transition state C−Br bending frequencies for $HCCl_2Br^+$ and repeated the fitting in order to determine if the arbitrarily fixed C−Br bending frequencies affect the derived Cl loss onset energy. Table 1 shows Br loss activation entropies derived from assuming various C−Br bending mode frequencies and the corresponding best-fit Cl loss activation entropies found by varying the transition state C−Cl bending frequencies.

The activation entropy is given by

$$\Delta S^\ddagger = R \ln \frac{Q^\ddagger}{Q} - \frac{U^\ddagger - U}{T} \qquad \text{(III)}$$

where the Q's are the vibrational partition functions for the transition state and the molecular ion and the U's are the internal energy at the desired temperature. The difference in the entropy of activation for the two channels is given by

$$\Delta\Delta S^\ddagger = R \ln\left(\frac{Q^\ddagger_{Cl}}{Q^\ddagger_{Br}}\right) - \frac{U^\ddagger_{Cl} - U^\ddagger_{Br}}{T} \qquad \text{(IV)}$$

The magnitude of $\Delta\Delta S^\ddagger$ indicates the relative rates of the competitive processes. The goodness-of-fit is determined by minimizing an error function

$$\text{Err} = 1 - \frac{\sum_i E_i S_i}{\sqrt{\sum_i E_i E_i \sum_i S_i S_i}} \qquad \text{(V)}$$

where E_i are the experimental points and S_i are the simulated points for the breakdown diagram.[31] The Err function ranges from 0 to 1, with 0 being a perfect fit with all E and S identical. It is evident from Table 1 that the error remains the same and the derived C−Cl ion bond energy is also invariant as we change the C−Br bending frequencies. Thus, a knowledge of the absolute value of the transition state bending modes is not important—only their difference is important.

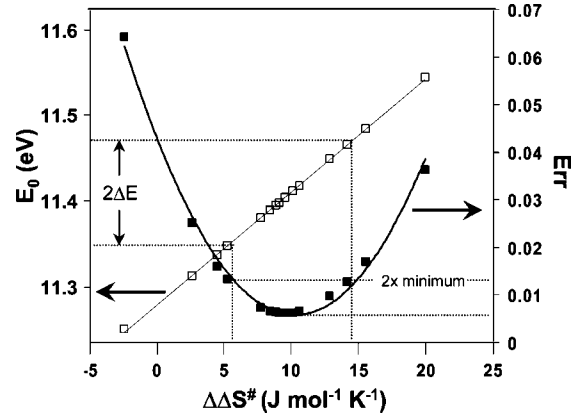

Figure 5. The Err (right axis, see text eq V) of the RRKM modeled fit to the second (Cl loss) dissociation onset from $CHCl_2Br^+$ as a function of the $\Delta\Delta S^\ddagger$ (see text) of the competing dissociations. The values of the dissociation barrier (left axis) at the points where the Err function reaches double its minimum determine the reported error limits.

The uncertainty associated with the first dissociation onset is determined by varying the E_0 until the value of Err in eq V is double the best-fit value, a rule of thumb that we have found corresponds well to a poor fit as judged by eye. In the case of the first dissociation, the uncertainty comes mainly from the resolution of the monochromator, which is about 10 meV. The uncertainty associated with the second dissociation onset, that of Cl loss, in the cases of the two mixed trihalomethanes is determined by finding the minimum in Err for a range of values of E_{Cl} by varying the frequencies of the C−Cl bending modes of the second transition state at each point. During this process, the vibrational frequencies of the first transition state and E_{Br} are kept constant. The value of E_{Cl} at which Err is double that of the global best-fit value determines the uncertainty. For $CHCl_2Br$, the results are summarized in Figure 5. The best-fit value of Err is 0.006, with an optimized onset of 11.425 eV. Multiplying that number by two gives 0.012, and the two corresponding optimized onsets are at 11.363 and 11.486 eV. Hence, the uncertainty is ±60 meV. Parts a and b of Figure 6 show the expanded $HCCl_2Br$ breakdown diagram in which the modeled fits at the edge of the uncertainty range are plotted. We consider these uncertainties to be at the 95% confidence limit.

Dissociation Onsets and Thermochemistry

The measured dissociation onsets are presented with the breakdown diagrams in Figures 1−4, and the appearance energies of all the dissociations are summarized in Figure 7.

We can now use these 0 K onsets to extract the 0 K heats of formation of all species starting with our well-established chloroform and less well established bromoform anchors. We determined the 0 K heat of formation from the 298 K value in the usual manner by

$$\Delta_f H^\circ_{0K}[CHCl_3] = \Delta_f H^\circ_{298K}[CHCl_3] - [H_{298} - H_0](CHCl_3) + [H_{298} - H_0]\left(C(s) + \frac{1}{2}H_2 + \frac{3}{2}Cl_2\right) \qquad \text{(VI)}$$

This yields a $\Delta_f H^\circ_{0K}[CHCl_3] = -98.4 \pm 1.3$ kJ mol^{-1} and a $\Delta_f H^\circ_{0K}[CHBr_3] = 81.0 \pm 6.0$ kJ mol^{-1}, values that will serve as anchors for the following calculations.

The application of Hess's law is shown in eq VII for reaction 1 in which we determine the 0 K heat of formation of $CHCl_2^+$, which is the only unknown species in the equation

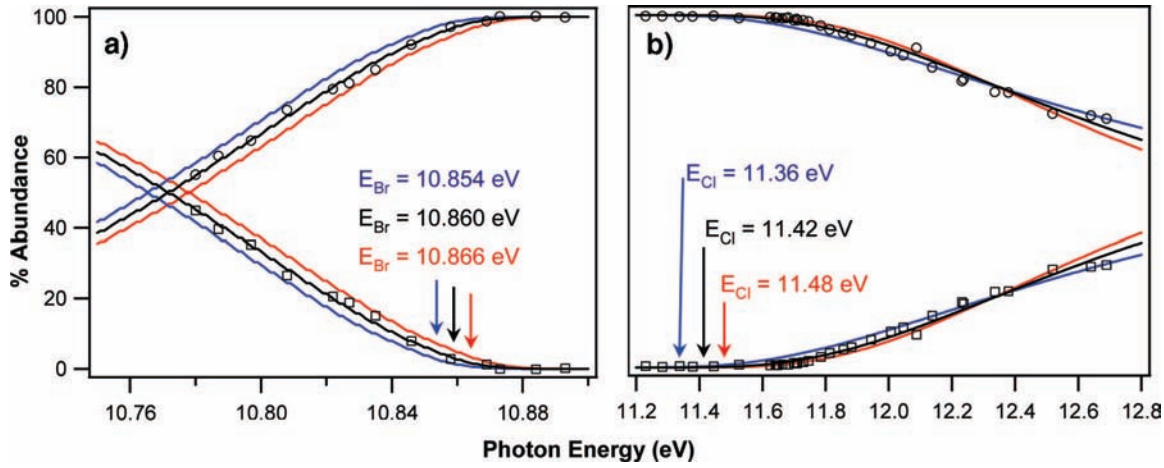

Figure 6. Best (black lines) and high (red) and low (blue) error limit fits of the $CHCl_2Br^+$ breakdown diagrams for (a) the first (Br loss) onset and (b) the second (Cl loss) onset. Error limits are (a) 6 and (b) 60 meV.

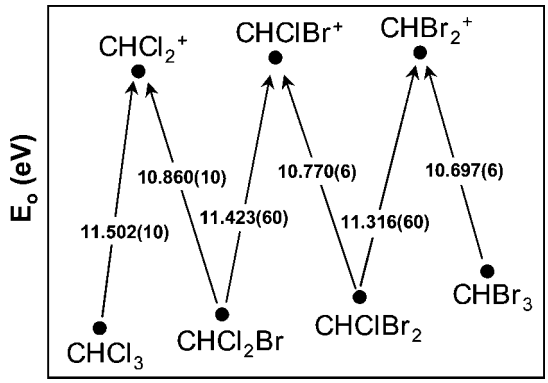

Figure 7. Dissociation onsets and their uncertainties (in eV) as determined in this study. Onsets are to the indicated ion and the appropriate radical ($Cl^\bullet$ or $Br^\bullet$, not shown for clarity).

TABLE 2: 0 K Heats of Formation and Uncertainties (in kJ mol^{-1}) Derived by Anchoring on Either Chloroform or Bromoform and the Weighted Averages of Those Values

	$\Delta_fH°$ (0 K) (kJ mol^{-1})		
	from $CHCl_3$	from $CHBr_3$	combined
$CHCl_3$	-98.4 ± 1.3^a	-98.6 ± 10.3	-98.4 ± 1.3
$CHCl_2^+$	891.8 ± 1.6	891.5 ± 10.2	891.7 ± 1.6
$CHCl_2Br$	-38.2 ± 1.9	-38.4 ± 10.2	-38.2 ± 1.9
$CHClBr^+$	944.4 ± 6.1	944.2 ± 8.4	944.3 ± 4.9
$CHBr_2Cl$	23.1 ± 6.1	22.9 ± 8.4	23.1 ± 4.9
$CHBr_2^+$	995.4 ± 8.4	995.1 ± 6.0	995.2 ± 4.9
$CHBr_3$	81.2 ± 8.4	81.0 ± 6.0^b	81.0 ± 4.9

[a] From ref 11. [b] See the Introduction.

$$E_0 = 1109.6 = \Delta_f H^\circ_{0K}[CHCl_2^+] + \Delta_f H^\circ_{0K}[Cl^\bullet] - \Delta_f H^\circ_{0K}[CHCl_3] \quad \text{(VII)}$$

The 0 K heats of formation of Cl and Br are 119.621 and 117.92 kJ mol^{-1}.[32] Once we have established the $CHCl_2^+$ energy we can obtain the $CHCl_2Br$ heat of formation from the Br loss reaction that produces the same $CHCl_2^+$ product. This is continued until we get to bromoform. As shown in Table 2, error propagation increases the uncertainties considerably, especially when the reaction involves the second onset, which is not established as precisely as the first onset. Nevertheless, it is remarkable that we reach a bromoform value of 81.2 ± 8.6 kJ mol^{-1} that agrees very well with the literature value of 81.0 kJ mol^{-1}.

If we now start the same process from bromoform, we can work our way backward until we reach chloroform. Because we reached essentially the literature value going one way, we will do the same going backward. However, it is important to note that each heat of formation derived from the chloroform anchor is independent of the derivation from the bromoform anchor. Consider the $CHCl_2Br$ heat; starting from chloroform, the derived value is dependent on the measured onsets of reactions 1 and 2, whereas starting from the bromoform the value is dependent on an entirely different set on onsets (reactions 3−6). Because these are essentially independent determinations (the determined E_{Br} does affect the determination of E_{Cl} in the $CHCl_2Br^+$ and $CHClBr_2^+$ dissociations, but negligibly so), they can be combined to establish values that are both more accurate and more precise.

The equations used to calculate these weighted averages and combined errors are listed as eqs VIII and IX below, respectively, where m_i are the independent measurements and e_i are the associated uncertainties.[33]

$$\text{average} = \frac{\sum_i \frac{m_i}{e_i^2}}{\sum_i \frac{1}{e_i^2}} \quad \text{(VIII)}$$

$$\text{combined error} = \sqrt{\frac{1}{\sum_i \frac{1}{e_i^2}}} \quad \text{(IX)}$$

Table 3 summarizes the derived 0 and 298 K heats of formation of the trihalomethanes.

Summary

The 0 K onsets of the six halogen loss reactions of the bromo and chloro trihalomethanes were determined by TPEPICO spectroscopy. The lowest energy onset from each of the four parent molecules was determined to within 10 meV, whereas the second onsets of the mixed trihalomethanes were determined to within 60 meV by RRKM modeling of the competing dissociations. These data allowed for two independent determinations of the heats of formations of $CHCl_3$, $CHBr_3$, $CHCl_2Br$, $CHClBr_2$, $CHCl_2^+$, $CHBr_2^+$, and $CHClBr^+$ by anchoring to either the literature value of chloroform or bromoform. The two heats determined for each molecule were in excellent agreement

TABLE 3: Summary of Trihalomethane Thermochemistry (in kJ mol^{-1})

			$\Delta_f H°_{298K}$	
	$\Delta_f H°_{0K}$	$H_{298} - H_0$	this work[a]	literature values
$CHCl_3$	-98.4 ± 1.1	14.2	-103.2	-103.2 ± 1.3[b]
$CHCl_2^+$	891.7 ± 1.5	11.2	888.5	888.9 ± 1.3[c]
$CHCl_2Br$	-38.2 ± 1.8	14.8	-50.1	-45 ± 20[d]
$CHClBr^+$	944.3 ± 4.9	11.6	933.8	
$CHClBr_2$	23.1 ± 4.9	15.4	4.1	10 ± 20[d]
$CHBr_2^+$	995.2 ± 4.9	12.0	977.4	987[e]
$CHBr_3$	81.0 ± 4.9	16.1	55.1	55.0 ± 6.0[e]

[a] 298 K uncertainties are identical to those reported at 0 K. [b] From ref 11. [c] From ref 10. [d] From ref 20. [e] Evaluated, see the Introduction.

with one another in all cases and were combined in order to increase the precision of the reported values. These are the first reported experimental heats of formation for $CHCl_2Br$, $CHClBr_2$, and $CHClBr^+$. The heats of formation of $CHCl_2Br$ and $CHClBr_2$ are in excellent agreement with previously reported estimated values, the heats of formation of $CHCl_3$, $CHBr_3$, and $CHCl_2^+$ are in excellent agreement with previously reported experimental values, and our reported $CHBr_2^+$ heat of formation is in reasonable agreement with the value that can be derived from the literature, but is far more precise.

Acknowledgment. We thank the U.S. Department of Energy, Office of Basic Energy Sciences, for financial support.

References and Notes

(1) Karton, A.; Rabinovich, E.; Martin, J. M. L.; Ruscic, B. *J. Chem. Phys.* **2006**, *125*, 144108−1–144108/17.

(2) Martin, J. M. L.; de Oliveira, G. *J. Chem. Phys.* **1999**, *111*, 1843–1856.

(3) Bomble, Y. J.; Vazquez, J.; Kallay, M.; Michauk, C.; Szalay, P. G.; Csaszar, A. G.; Gauss, J.; Stanton, J. F. *J. Chem. Phys.* **2006**, *125*, 064108−1–064108/8.

(4) Harding, M. E.; Vazquez, J.; Ruscic, B.; Wilson, A. K.; Gauss, J.; Stanton, J. F. *J. Chem. Phys.* **2008**, *128*, 114111−1–114111/15.

(5) Tajti, A.; Szalay, P. G.; Csaszar, A. G.; Kallay, M.; Gauss, J.; Valeev, E. F.; Flowers, B. A.; Vazquez, J.; Stanton, J. F. *J. Chem. Phys.* **2004**, *121*, 11599–11613.

(6) Ruscic, B.; Pinzon, R. E.; Morton, M. L.; Srinivasan, N. K.; Su, M.-C.; Sutherland, J. W.; Michael, J. V. *J. Phys. Chem. A* **2006**, *110*, 6592–6601.

(7) Ruscic, B.; Pinzon, R. E.; Morton, M. L.; Laszevski, G.; Bittner, S. J.; Nijsure, S. G.; Amin, K. A.; Minkoff, M.; Wagner, A. F. *J. Phys. Chem. A* **2004**, *108* (45), 9979–9997.

(8) Lago, A. F.; Kercher, J. P.; Bodi, A.; Sztáray, B.; Miller, B. E.; Wurzelmann, D.; Baer, T. *J. Phys. Chem. A* **2005**, *109*, 1802–1809.

(9) Lago, A. F.; Baer, T. *J. Phys. Chem. A* **2006**, *110*, 3036–3041.

(10) Lago, A.; Baer, T. *Int. J. Mass Spectrom.* **2006**, *252*, 20–25.

(11) Manion, J. A. *J. Phys. Chem. Ref. Data* **2002**, *31* (1), 124–165.

(12) Hu, A. T.; Sinke, G. C. *J. Chem. Thermodyn.* **1969**, *1*, 507–513.

(13) Lazarou, Y. G.; Papadimitriou, V. C.; Vassileios, C.; Prosmitis, A. V.; Papagiannakopoulos, P. *J. Phys. Chem. A* **2002**, *106*, 11502–11517.

(14) Wagman, D. D.; Evans, W. H. E.; Parker, V. B.; Schum, R. H.; Halow, I.; Mailey, S. M.; Churney, K. L.; Nuttall, R. L. The NBS Tables of Chemical Thermodynamic Properties. J. Phys. Chem. Ref. Data; Vol. 11, Suppl. 2; NSRDS; U.S. Government Printing Office: Washington, DC, 1982.

(15) Pedley, J. B. *Thermochemical Data and Structures of Organic Compounds;* Thermodynamics Research Center: College Station, 1994.

(16) Papina, T. S.; Kolesov, V. P.; Golovanova, Y. G. *Russ. J. Phys. Chem. (Engl. Transl.)* **1982**, *56*, 1666–1669.

(17) Oren, M.; Iron, M. A.; Burcat, A.; Martin, J. M. L. *J. Phys. Chem. A* **2004**, *108*, 7752–7761.

(18) Marshall, P.; Srinivas, G. N.; Schwartz, M. *J. Phys. Chem. A* **2005**, *109* (28), 6371–6379.

(19) Wang, L. *J. Phys. Chem. A* **2008**, *112*, 4951–4957.

(20) Gurvich, L. V.; Veyts, I. V.; Alcock, C. B. *Thermodynamic Properties of Individual Substances*, 4th ed.; Hemisphere Publishing Co.: Bristol, PA, 1991.

(21) Andrews, L.; Dyke, J. M.; Jonathan, N.; Keddar, N.; Morris, A. *J. Phys. Chem.* **1984**, *88* (10), 1950–1954.

(22) Holmes, J. L.; Lossing, F. P. *J. Am. Chem. Soc.* **1988**, *110*, 7343–7345.

(23) Seetula, J. A. *Phys. Chem. Chem. Phys.* **2003**, *5*, 849–855.

(24) Baer, T.; Li, Y. *Int. J. Mass Spectrom.* **2002**, *219*, 381–389.

(25) Sztáray, B.; Baer, T. *Rev. Sci. Instrum.* **2003**, *74*, 3763–3768.

(26) Baer, T.; Sztáray, B.; Kercher, J. P.; Lago, A. F.; Bodi, A.; Scull, C.; Palathinkal, D. *Phys. Chem. Chem. Phys.* **2005**, *7*, 1507–1513.

(27) Frisch, M. J.; Trucks, G. W.; Schlegel, H. B.; Scuseria, G. E.; Robb, M. A.; Cheeseman, J. R.; Montgomery, J. A., Jr.; Vreven, T.; Kudin, K. N.; Burant, J. C.; Millam, J. M.; Iyengar, S. S.; Tomasi, J. J.; Barone, V.; Mennucci, B.; Cossi, M.; Scalmani, G.; Rega, N.; Petersson, G. A.; Nakatsuji, H.; Hada, M.; Ehara, M.; Toyota, K.; Fukuda, R.; Hasegawa, J.; Ishida, M.; Nakajima, T.; Honda, Y.; Kitao, O.; Nakai, H.; Klene, M.; Li, X.; Knox, J. E.; Hratchian, H. P.; Cross, J. B.; Adamo, C.; Jaramillo, J.; Gomperts, R.; Stratmann, R. E.; Yazyev, O.; Austin, A. J.; Cammi, R.; Pomelli, C.; Ochterski, J. W.; Ayala, P. Y.; Morokuma, K.; Voth, A.; Salvador, P.; Dannenberg, J. J.; Zakrzewski, V. G.; Dapprich, S.; Daniels, A. D.; Strain, M. C.; Farkas, O.; Malick, D. K.; Rabuck, A. D.; Raghavachari, K.; Foresman, J. B.; Ortiz, J. V.; Cui, Q.; Baboul, A. G.; Clifford, S.; Cioslowski, J.; Stefanov, B. B.; Liu, G.; Liashenko, A.; Piskorz, P.; Komaromi, I.; Martin, R. L.; Fox, D. J.; Keith, T.; Al-Laham, M. A.; Peng, C. Y.; Nanayakkara, A.; Challacombe, M.; Gill, P. M. W.; Johnson, B.; Chen, W.; Wong, M. W.; Gonzalez, C.; Pople, J. A. Gaussian 03, revision C.02; Gaussian, Inc.: Pittsburgh, PA, 2004.

(28) Werner, A. S.; Tsai, B. P.; Baer, T. *J. Chem. Phys.* **1974**, *60*, 3650–3657.

(29) Tsai, B. P.; Baer, T.; Werner, A. S.; Lin, S. F. *J. Phys. Chem.* **1975**, *79*, 570–574.

(30) Baer, T.; Hase, W. L. *Unimolecular Reaction Dynamics: Theory and Experiments*; Oxford University Press: New York, 1996.

(31) Sztáray, B.; Baer, T. *J. Am. Chem. Soc.* **2000**, *122*, 9219–9226.

(32) Chase, M. W. *NIST−JANAF Thermochemical Tables*, 4th ed.; American Institute of Physics: New York, 1998.

(33) Bevington, P. R.; Robinson, D. K. *Data Reduction and Error Analysis for the Physical Sciences*; McGraw Hill: Boston, MA, 2003.

JP8056459